Carbohydrate Polymers 92 (2013) 206–213

Contents lists available at SciVerse ScienceDirect

Carbohydrate Polymers

journal homepage: www.elsevier.com/locate/carbpol

# Preparation and properties of aligned poly(3-hydroxybutyrate-*co*-3-hydroxyvalerate)/cellulose nanowhiskers composites

Elena Ten [a], Long Jiang [b,*], Michael P. Wolcott [a,**]

[a] *Composite Materials and Engineering Center, Washington State University, Pullman, WA 99164-1806, United States*
[b] *Department of Mechanical Engineering, North Dakota State University, Fargo, ND 58108-6050, United States*

ARTICLE INFO

*Article history:*
Received 29 May 2012
Received in revised form 14 August 2012
Accepted 15 September 2012
Available online 24 September 2012

*Keywords:*
Anisotropic nanocomposite
Cellulose nanowhiskers
Poly(3-hydroxybutyrate-*co*-3-hydroxyvalerate)
Unidirectional composite

ABSTRACT

In this study a unidirectionally aligned cellulose nanowhisker (CNW) composite was developed. CNW in poly(3-hydroxybutyrate-*co*-3-hydroxyvalerate) (PHBV) matrix was aligned using an external electric field and the morphology and mechanical properties of the resultant anisotropic composites were studied. PHBV films with 1.5–7 wt% of CNWs were manufactured using solution casting. A DC electric field of 56.25 kV/m was applied during solvent evaporation. Both microstructural and mechanical analyses were performed to study the orientation of CNWs in the films. Mechanical properties of the samples were tested at 0°, 15°, 30°, 45° and 90° with respect to electric field direction by a dynamic mechanical analyzer (DMA). DMA results showed that CNW concentration has a strong influence on the degree of CNW alignment. The electric field was effective in aligning CNWs up to 4 wt% CNW concentration. The samples with higher concentrations showed virtually isotropic behavior, due to significantly enhanced restraints on CNW mobility. The restrains were attributed to CNW/CNW and CNW/polymer interactions. Rheological results confirmed the enhance restraints.



## 1. Introduction

Polyhydroxyalkanoates (PHAs) are a family of biodegradable polyesters produced by bacteria as a carbon and energy storage through natural biosynthesis (Ballard, Holmes, & Senior, 1987). PHAs show mechanical performance and glass transition temperature comparable to isotactic polypropylene (Pirrotta, 1993). Poly(3-hydroxybutyrate-*co*-3-hydroxyvalerate) (PHBV) is a copolymer of hydroxybutyrate (HB) and hydroxyvalerate (HV) and is a representative polymer from PHA family. The incorporation of HV increases the toughness of pure PHB by reducing its crystallization.

CNWs are needle-like elementary crystallites which constitute the cell walls of plants and the shells of some sea creatures (e.g. tunicin). Depending upon their origins and isolation methods, CNWs exhibit a Young's modulus of 57–143 GPa (Matsuo, Sawatari, Iwai, & Ozaki, 1990; Rusli & Eichhorn, 2008; Sakurada, Nukushina, & Ito, 1962; Stucova, Davies, & Eichhorn, 2005), a typical length of 200–400 nm, and a diameter smaller than 10 nm (Bondeson, Mathew, & Oksman, 2006). Such properties make CNWs an ideal nano-reinforcement material for polymer matrixes.

We have systematically studied the preparation and properties of PHBV/CNW composites (Jiang, Morelius, Zhang, Wolcott, & Holbery, 2008; Ten, Jiang, Bahr, Li, & Wolcott, 2012; Ten, Jiang, & Wolcott, 2012; Ten, Turtle, Bahr, Jiang, & Wolcott, 2010). Our results showed that PHBV reinforced with homogeneously distributed CNWs could be prepared by solution casting. Significant improvements in tensile strength, Young's modulus, toughness, dynamic modulus were observed (Ten et al., 2010). Thermal, mechanical, dielectric, and dynamic mechanical properties exhibited abrupt transitions at 2.3–2.9 wt% CNW concentrations due to the change in CNW dispersion state (Ten, Jiang, Bahr, et al., 2012). CNWs also played an important role in PHBV crystallization (Ten, Jiang, Bahr, et al., 2012; Ten et al., 2010). Depending on its concentration, CNW could either improve heterogeneous nucleation of PHBV (at low CNW concentrations) or hinder spherulite growth of the polymer (at high CNW concentrations) (Ten, Jiang, & Wolcott, 2012).

The incorporation of fibers into polymer matrixes causes anisotropicity of the fiber composites. The ability to regulate fiber orientation is desirable in order to control the properties of the composite and expand their application areas. Attempts have been made to produce oriented CNW nanocomposites. Three

* Corresponding author. Tel.: +1 701 231 9512.
** Corresponding author. Tel.: +1 509 335 6392; fax: +1 509 335 5077.
*E-mail addresses:* long.jiang@ndsu.edu (L. Jiang), wolcott@wsu.edu (M.P. Wolcott).

0144-8617/$ – see front matter © 2012 Elsevier Ltd. All rights reserved.
http://dx.doi.org/10.1016/j.carbpol.2012.09.033

forces, i.e. mechanical (Cranston & Gray, 2003; Edgar & Gray, 2003; Nishiyama, Kuga, Wada, & Okano, 1997), magnetic (Cranston & Gray, 2006; Kimura et al., 2005; Kvien & Oksman, 2007; Li et al., 2010; Sugiyama, Chanzy, & Maretg, 1992) and electric forces (Bordel, Putaux, & Heux, 2006; Habibi, Heim, & Douillard, 2008) were used to align CNW fibers. CNWs were oriented radially in layer-by-layer (LbL) self-assembled polyelectrolyte multilayer films using spin-coating (Cranston & Gray, 2003). Linearly oriented films were obtained by shearing a drop of concentrated aqueous nanocrystal suspension along mica or polystyrene surfaces (Edgar & Gray, 2003). In another study (Nishiyama et al., 1997), a vial containing aqueous CNW suspension was kept in a horizontal position. The vial was rotated around its axis at 500 rpm at room temperature. The resulting film was found to be highly anisotropic and brittle in the direction perpendicular to the fiber orientation.

Magnetic fields have been reported to produce good CNW orientations. Sugiyama et al. (1992) aligned CNWs using a magnetic field of 7 T. Later, preliminary experiments relevant to layer-by-layer self-assembly of oriented cellulose nanocrystals were performed also in a 7 T magnetic field (Cranston & Gray, 2006). First attempt to orient CNWs in polymeric matrix was reported by Kvien and Oksman (2007). CNWs (2 wt%) were incorporated in a polyvinyl alcohol matrix using solution casting with water as a solvent. The water evaporated while a ~7 T homogeneous magnetic field was applied. Dynamic mechanical thermal analysis (DMTA) showed that the storage modulus of the nanocomposite was ~47% higher in the transverse direction than in the magnetic field direction, an indication of CNW orientation in the transverse direction (Kvien & Oksman, 2007). The orientation was attributed to CNW's different diamagnetic susceptibility in its axial and transverse directions (Kimura et al., 2005).

Applying electric field is another alternative method to align CNWs. Bordel et al. (2006) successfully demonstrated for the first time the ability of electric fields to align ramie cellulose fibers at macroscopic and colloidal levels in apolar organic solvents. However, this pioneer study did not investigate the effects of the electric field (frequency and amplitude) on the fiber orientation. Recently, Habibi et al. (2008) reported a highly reproducible, efficient and quick method to create anisotropic films from aqueous suspensions of tunicate and ramie CNWs. A high degree of fiber orientation was observed under the electric field of 2 kV/cm and above.

Literature study has shown that the development of oriented CNW composites is still in its early stage. Producing polymer/CNWs nanocomposites with desirable polymer matrix material and CNW orientations remains a technical and scientific challenge. Comprehensive property characterizations of the oriented composites are still lacking. In this study, we developed a method to prepare PHBV/CNWs nanocomposite with unidirectional CNW orientation. The effects of CNW content and orientation angle on the dynamic mechanical properties of the composites were evaluated. This study provided a new anisotropic CNW-reinforced biodegradable composite which showed great potential in many applications.

## 2. Experimental

### 2.1. Materials

PHBV with 12 mol% content of hydroxyvalerate (HV) was supplied by Metabolix Inc. *N*,*N*-dimethylformamide (DMF) and NaOH were purchased from Acros Organics (Atlanta, GA). Microcrystalline cellulose (MCC) was obtained from Avicel (Type PH-102). Sulfuric acid (96 wt%) was purchased from J.T. Baker. PHBV was dried at 80 °C in a convection oven overnight prior to use.

### 2.2. CNW preparation

Sulfuric acid was diluted to 64 wt% concentration. MCC (1 g per 9.8 ml of the acid) was added and vigorously stirred at 44 °C for 2 h. Then the suspension was diluted to about one-tenth of its original acid concentration to stop the reaction. The acid in the solution was removed by repeated centrifugation (Sorvall, 5000 rpm for 5 min) until the supernatant was turbid. The supernatant (CNW suspension) was collected and dialyzed against deionized water for 4–5 days to remove remaining acid (dialysis tube from Spectrum Laboratories Inc., cutoff molecular weight 12,000–14,000 Da). After the CNW suspension reached a constant pH value, it was removed from the dialysis tubes and neutralized with 1 wt% NaOH solution. The neutralized suspension was condensed at 80 °C using a Büchi Rotavapor (R-200) until the CNW concentration reached 2 wt%.

### 2.3. Preparation of aligned PHBV/CNW nanocomposites

Various volumes of the condensed CNW suspension were added drop-wise into 40 ml of DMF under continuous stirring. Water was evaporated from the mixture at 80 °C for an hour (DMF boiling temperature 153 °C) to obtain CNW/DMF suspension. Depending on the desired CNW content in the final PHBV/CNWs composites, different weights of PHBV were dissolved in the suspension under continuous stirring. The dispersion of CNWs in the suspension was improved by sonication for 5 min. The suspension was cast on a clean glass substrate (10 cm × 16 cm) which was placed between two ϕ10 cm circular electrodes (Fig. 1). A 9 kV voltage was applied on the electrodes (16 cm apart), which resulted in a maximum electric field of 56.25 kV/m (9 kV/0.16 m) between the electrodes. It is worth noting that the dielectric constant of DMF is high (36.7 at 25 °C). Therefore, the actual magnitude of the electric field was lower within the volume of DMF. The suspension on the glass substrate was heated with a lamp to accelerate DMF evaporation. The temperature of the suspension was measured to be 80 °C. Both the electric field and heat were applied continuously until the film was completely dry (3–4 h). Because the electrodes were relatively small compared to the size of the cast sample, non-uniform electric field across the sample could exist. To counter this effect, all test specimens in this study were cut from the center of the films where the electric field was the strongest.

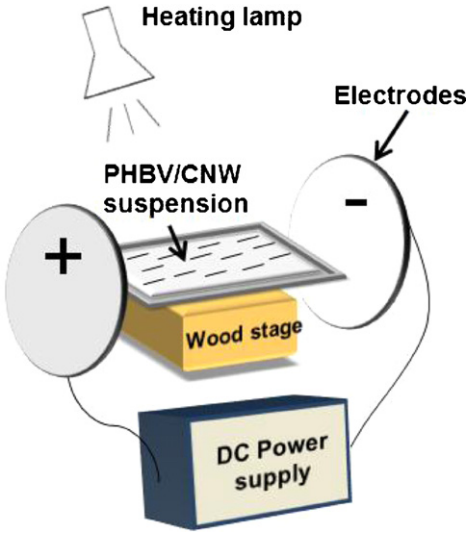


**Fig. 1.** The device used to prepare unidirectional PHBV/CNW composite film using an electric field.

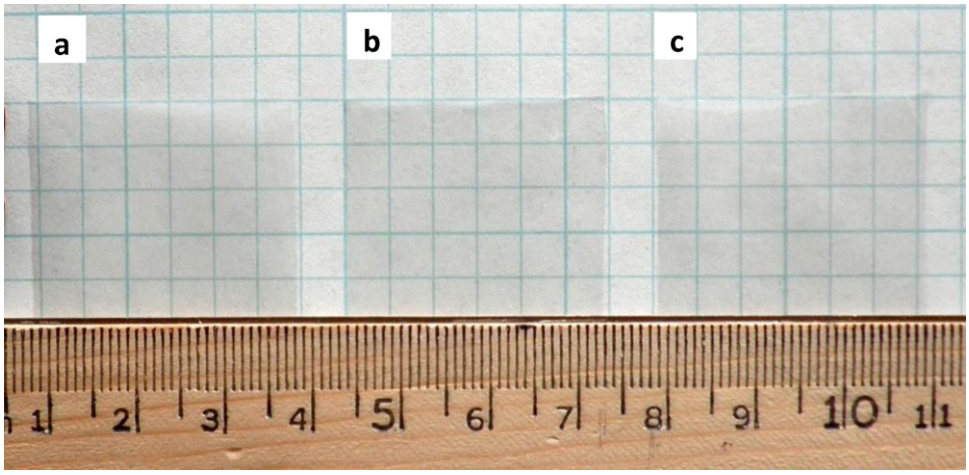


**Fig. 2.** Photographs of PHBV/CNW composite films: (a) neat PHBV; (b) PHBV/3% CNW; and (c) PHBV/7% CNW.

The final PHBV/CNW films appeared transparent (Fig. 2) and had a thickness between 15 and 30 μm. DMF content of the obtained films was measured to be less than 2 wt% through vacuum drying.

### 2.4. Characterization

#### 2.4.1. Atomic force microscopy (AFM)

Morphology of CNWs was investigated using AFM. The tests were performed in tapping mode using a Veeco Multimode AFM equipped with a NanoScope IIIa controller (Digital Instruments Inc.). Prior to the tests, a drop of CNW suspension in water was deposited on freshly cleaved mica surfaces. The solution was completely dried by natural evaporation. The dried sample was scanned in air using Si tips (Digital Instruments Inc.) with a resonance frequency of ca. 330 kHz. The scan rate was 0.5 Hz.

#### 2.4.2. Transmission electron microscopy (TEM)

The shape and size of CNWs were studied using a Philips CM-200 TEM operating at 200 kV. Similar to the sample preparation method used for AFM, a drop of CNW water suspension was introduced onto a formvar-coated nickel grid (300 mesh), rinsed with double-deionized water and dried naturally. TEM images of CNWs were acquired without any sample staining.

To study the morphology of the composite films, small pieces of PHBV/CNW films were embedded in acrylic resin (London Resin Company Ltd.) and cured at elevated temperature overnight. Thin sections (~50 nm) of the films were cut with a freshly prepared glass knife in the direction parallel to the film surface using a Reichert-Jung ultramicrotome (Reichert-Jung, Inc., Buffalo, NY). The sections were placed on formvar-coated nickel grids and then stained with 2% uranyl acetate for 90 min.

#### 2.4.3. Dynamic mechanical analysis (DMA)

DMA was conducted in tension mode on a Tritec 2000 DMA at 1 Hz to examine thermal dynamic properties of the films. DMA samples (10 mm × 6.5 mm) were cut from the center of the PHBV/CNW composite films. Dynamic strain sweep was first performed to determine linear viscoelastic range of the samples. Then the samples were tested from −40 °C to +80 °C at 5 °C/min heating rate with a strain of 0.02%. To study the effect of fiber orientation angle $\theta$ (Fig. 3) on the storage modulus of the composites, the samples were cut at 0°, 15°, 30°, 45° and 90° with respect to the direction of the applied electric field. Ten replicates were tested for each orientation angle $\theta$. The storage moduli $E'$ of the samples were compared at temperatures below (−20 °C) and above (60 °C) the glass transition temperature of PHBV (ca. 25 °C).

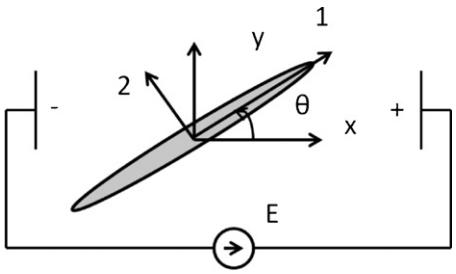


**Fig. 3.** Schematic showing the orientation angle of CNW in the electric field. $E$, electric field (kV/m); $\theta$, orientation angle (°).

#### 2.4.4. Rheology test

A strain-controlled rheometer (RDA III, Rheometric Scientific) was used to measure dynamic rheological properties and viscosity of PHBV/CNW composites. The measurements were performed at 175 °C using a pair of parallel discs (25 mm diameter). The gap between the two discs was 0.5 mm. PHBV/CNW films were stacked and melted at 175 °C in the geometry. Care was taken to make sure there were no air bubbles in the sample melt. A strain sweep test was first performed to determine the linear viscoelastic region of the composites and a shear strain of 0.6% was chosen for all subsequent frequency sweep tests. The frequency was varied from 1 to 500 rad/s.

## 3. Results and discussion

### 3.1. Morphology of CNWs

The morphology of CNWs is shown in TEM and AFM micrographs (Fig. 4). Individual nanowhiskers can be identified from the TEM image (Fig. 4a). The concentration of the CNWs in the AFM micrographs appears much higher than in the TEM because of their different sample preparation methods. In TEM the nickel grid was rinsed by trickling deionized water over the grid after an initial drop of CNW suspension was deposited. This operation reduced CNW concentration significantly and allowed the imaging of individual CNWs. Thus, CNW dimensions were calculated based on the TEM micrographs. The aspect ratio of the nanowhiskers was determined based on the measurement of 300 individual whiskers using ImageJ software (National Institute of Health). An average CNW diameter and length were determined to be 12.32 ± 4.0 nm and 221.88 ± 47.9 nm. CNW diameter and length were also calculated from the TEM micrographs of PHBV/CNW films (Fig. 6a–c). Values of 12.34 ± 3.7 nm and 218.05 ± 52.3 nm

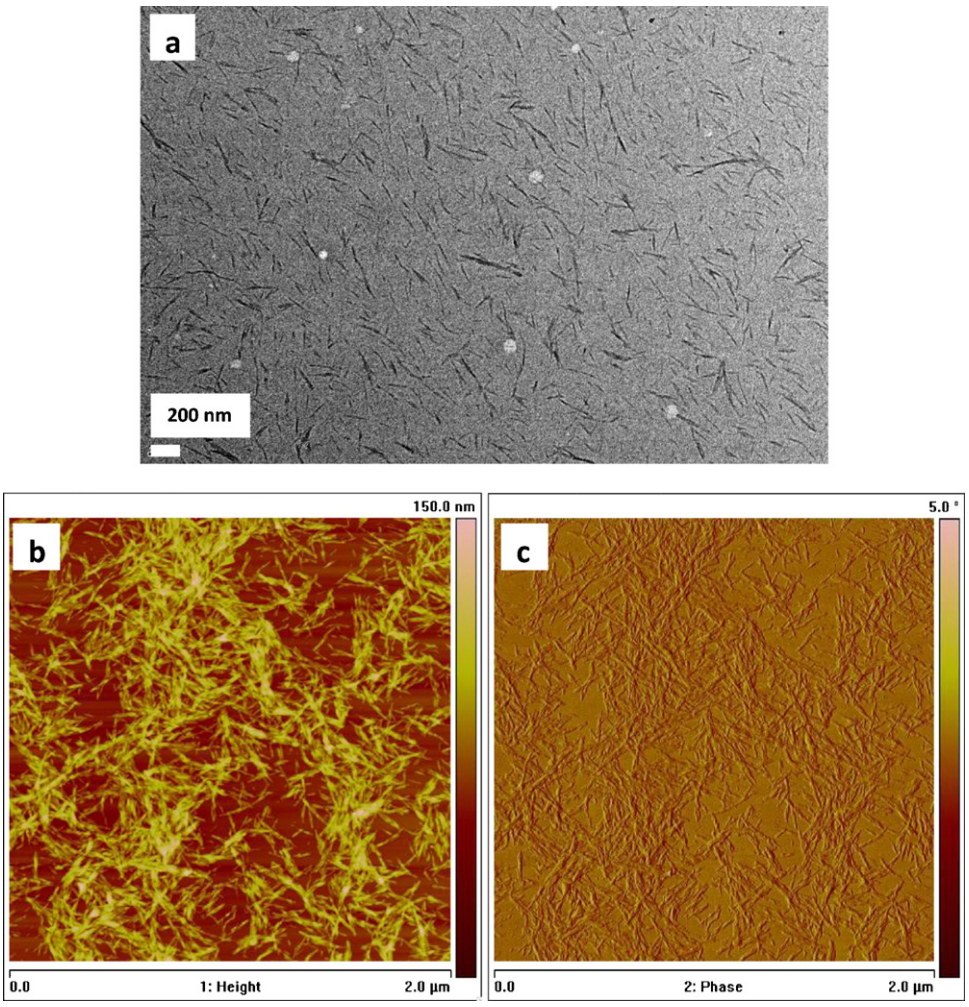


**Fig. 4.** Morphology of CNWs: (a) TEM micrograph; (b) AFM topography; and (c) AFM phase image.

were obtained for the diameter and length, respectively. The values are close to those obtained from the CNW suspension, implying that CNWs were homogeneously dispersed the PHBV matrix and no significant fiber fractures occurred during the film preparation process.

The aspect ratio ($L/d$) of CNWs was fitted to a probability density function (pdf) of the two-parameter Weibull distribution (Fig. 5). The Weibull distribution is a probabilistic model that allows describing the size distribution of particles (Rosin & Rammler, 1933). The probability density function (pdf) can be described as:

$$f(x) = \frac{\beta}{\alpha}\left(\frac{x}{\alpha}\right)^{\beta-1} e^{-(x/\alpha)^{\beta}}; \quad (1)$$

where $\alpha$ and $\beta$ are scale and shape parameters, respectively. Both $\alpha$ and $\beta$ are positive numbers.

The Weibull distribution was plotted to fit experimental CNW aspect ratio distribution (Fig. 5). $\alpha = 20.26$ and $\beta = 2.04$ were obtained under the condition of $R^2 = 0.947$.

The average ($\bar{L}/d$) value can be determined as $E(x)$ that is given by:

$$E(x) = \alpha\Gamma\left(1 + \frac{1}{\beta}\right) = 17.95; \quad (2)$$

The experimental average aspect ratio based on 300 measurements was $18.01 \pm 7.5$, which is close to the model predicted value of 17.95. Therefore, it can be concluded that the aspect ratio distribution of CNWs can be accurately described by a two-parameter Weibull distribution.

### 3.2. Microstructure of aligned PHBV/CNW composites by TEM

The alignment of CNWs in the PHBV matrix was studied using TEM (Fig. 6). It can be seen that for the samples with low CNW

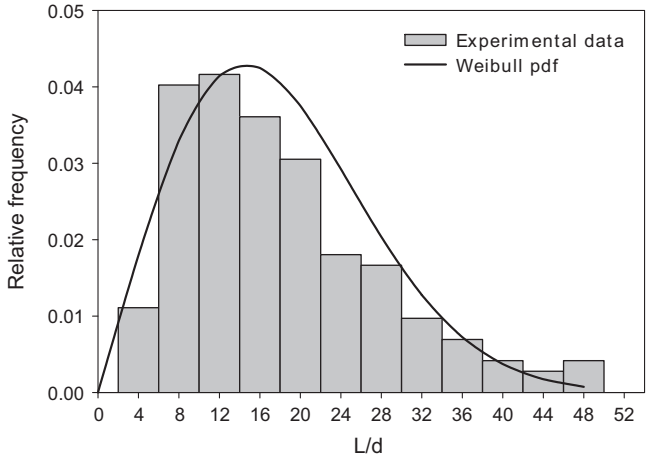


**Fig. 5.** CNW aspect ratio distribution fitted with the Weibull probability density function.

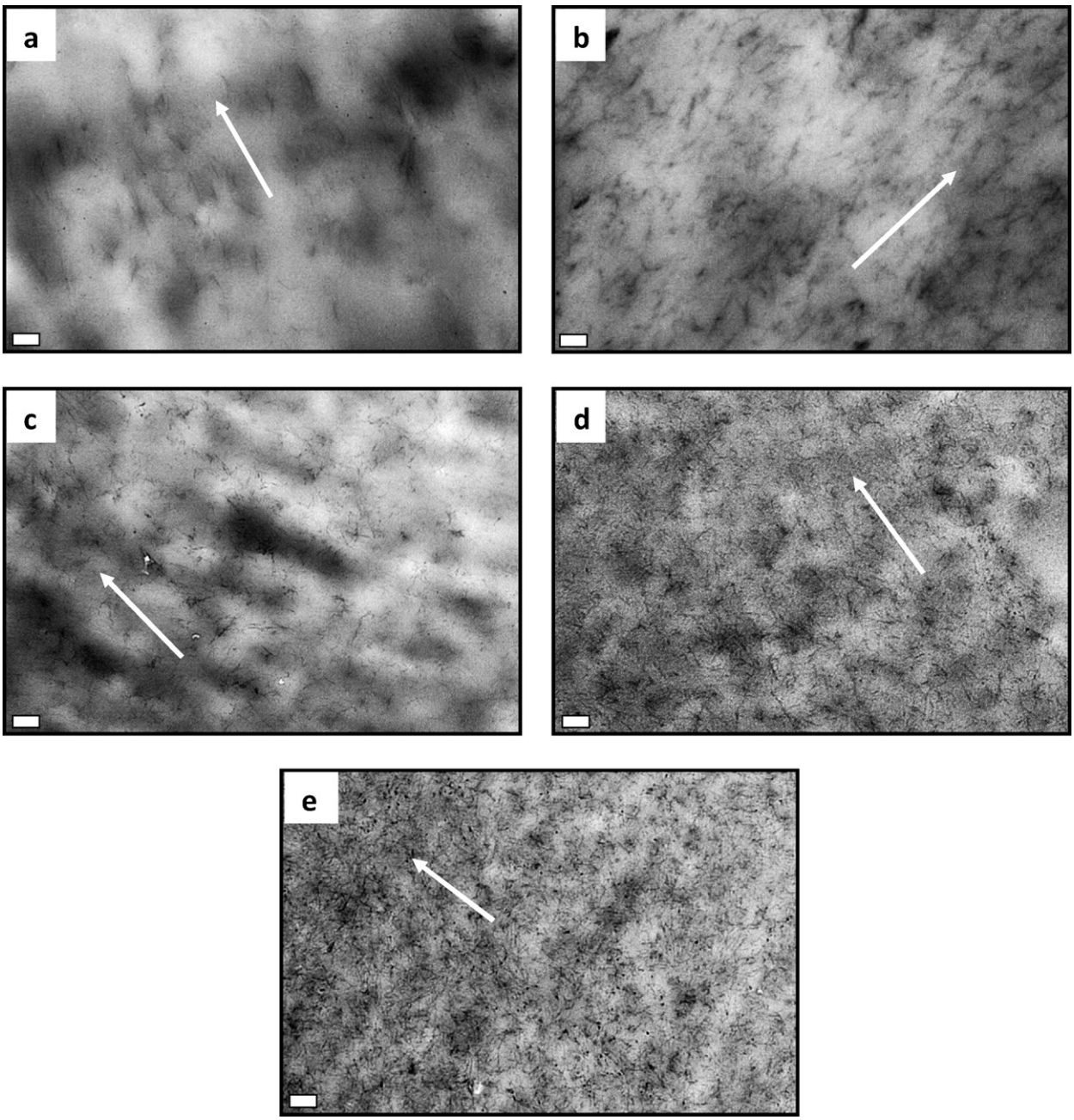


**Fig. 6.** TEM images of PHBV/CNW composites: (a) PHBV/1.5 CNW; (b) PHBV/2 CNW; (c) PHBV/3 CNW; (d) PHBV/4 CNW; and (e) PHBV/5 CNW. Scale bars represent 200 nm. Arrows show the direction of applied electric field.

concentrations, i.e. 1.5% and 2% (Fig. 6a and b), CNWs were aligned along the direction of the applied electric field. Because of the structural anisotropy of CNWs, the dipole moment of CNWs in their axial direction is stronger than that in the transverse direction. Therefore, cellulose nanowhiskers could be aligned along the direction of the electric field if the alignment is not hindered by their surrounding environment. At 3% and 4% CNW concentrations, the nanowhiskers showed lower degrees of fiber orientation compared to the 1.5% and 2% samples (Fig. 6c and d). At 5% concentration, no preferential fiber orientation could be observed (Fig. 6e). Although similar levels of field-induced dipolar interactions existed in all the composites, the orientation of the fibers was restrained presumably due to strong fiber–fiber and fiber–matrix interactions at high fiber concentrations. This presumption was confirmed by rheological and dynamic mechanical tests on the samples containing 0–5 wt% CNWs.

### 3.3. Melt viscosity of PHBV/CNW composites

Fig. 7 shows the complex viscosity ($\eta^*$) of the samples plotted as a function of frequency. $\eta^*$ increased with the increasing CNW content within the whole frequency range (1–500 rad/s). The increase was especially significant in the terminal zone (i.e. low frequency zone) (Fig. 7). In this region, the neat PHBV showed a Newtonian plateau – a constant viscosity regardless of the frequency. The plateau disappeared even when the lowest content of CNWs (1.5 wt%) was added. All the samples containing CNWs displayed a significant shear-thinning behavior in the terminal zone.

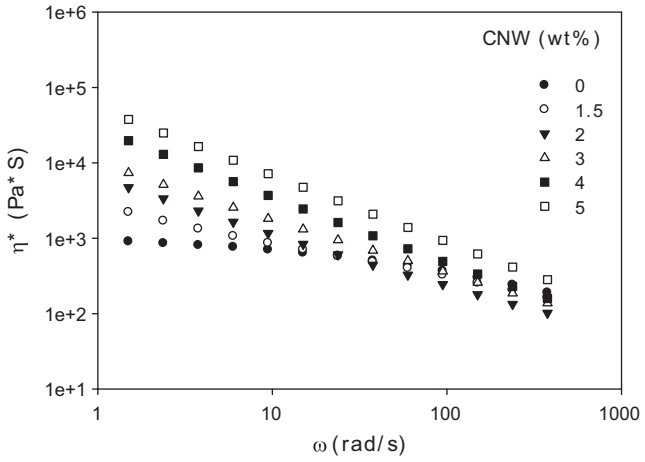


**Fig. 7.** Complex viscosity $\eta^*$ vs. angular frequency of PHBV/CNW composites.

The disappearance of the Newtonian behavior and the significant increase in the complex viscosity within the terminal zone is a clear indication of the alteration of PHBV chain dynamics after the incorporation of CNWs. Fiber–fiber and fiber–matrix interactions played influential roles in PHBV chain mobility. Chain movements were refrained under these interactions and chain relaxation was hindered. Physical network structure could be formed under the influence of these interactions and the progressive destruction of the structure with increasing shear rate led to the shear thinning behavior in the terminal zone. In addition, the shear thinning could also be partially attributed to the flow-induced alignment of CNWs under the shear flow of the rheological tests (Marcovich, Auad, Bellesi, Nutt, & Aranguren, 2006). This observation was previously described for cellulose aqueous suspensions (Azizi Samir, Alloin, Sanchez, Kissi, & Dufresne, 2004; Ebeling et al., 1999).

The complex viscosities determined at 1.5 rad/s for all the composites were plotted as a function of CNW concentration in Fig. 8. It was evident that the viscosity increased with increasing CNW concentration. The increase in melt viscosity appears to be commonly observed in both thermoplastics and thermosets based cellulosic nanocomposites (Dubief, Samain, & Dufresne, 1999; Habibi & Dufresne, 2008; Mabrouk, Magnin, Belgacem, & Boufi, 2011; Marcovich et al., 2006). Furthermore, the rate of increase suddenly improved when the concentration exceeded ~3%, a possible indication of CNW percolation.

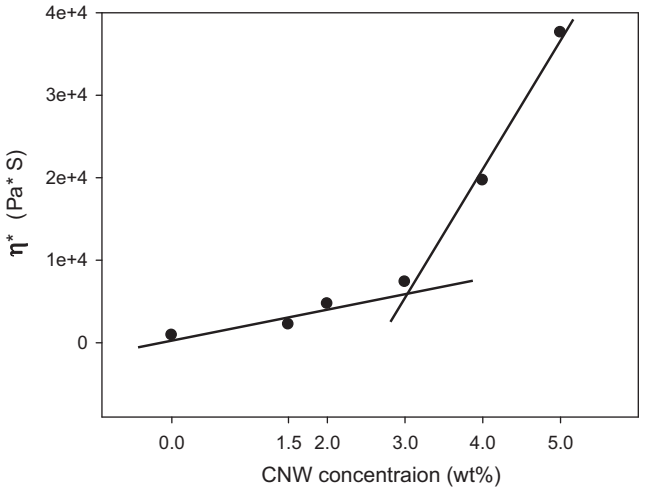


**Fig. 8.** The effect of CNW concentration on complex viscosity $\eta^*$ of PHBV/CNW composites at $\omega = 1.5$ rad/s.

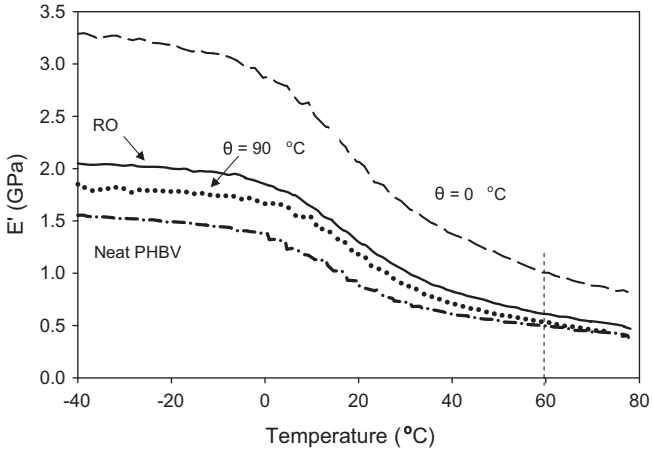


**Fig. 9.** Storage modulus as a function of temperature of neat PHBV, randomly oriented (RO) PHBV/CNW, and aligned PHBV/CNW (measured at 0° and 90° orientation angle. CNW content: 1.5 wt%.

### 3.4. Dynamic mechanical properties of aligned PHBV/CNW composites

The dynamic mechanical properties of the nanocomposites were measured at $\theta = 0°$, 15°, 30°, 45° and 90° with respect to the direction of the applied electric field. Representative curves of the storage modulus $E'$ as a function of temperature for the oriented PHBV/1.5% CNW samples tested at the fiber axial direction ($\theta = 0°$) and the transverse direction ($\theta = 90°$) are shown in Fig. 9. $E'$ of neat PHBV and a non-oriented control sample (random CNW orientation) is also shown for comparison. The control sample was prepared under the same condition as the oriented samples except that no electric field was applied. The decrease of $E'$ between 5 and 60 °C corresponded to the glass transition of PHBV. The large difference of $E'$ in the longitudinal and transverse directions indicated high anisotropy of the aligned films. For instance, $E'$ in the longitudinal direction was 77% (at −10 °C) and 87% (at 60 °C) higher than that in the transverse direction. The magnitude of $E'$ of all the samples followed the order of 0° > RO > 90° > neat PHBV, demonstrating directional reinforcing effects of the oriented cellulose nanofibers.

$E'$ measured at different angles for the aligned composites comprising various concentrations of CNWs are compared in Fig. 10. In general, higher CNW concentration led to higher $E'$ and lower slopes of the lines (i.e. lower difference of $E'$ between different angles). The degree of anisotropy of the composites can by indicated by the percentage difference between $E'$ in the axial ($\theta = 0°$) and transverse ($\theta = 90°$) directions using Eq. (3):

$$\text{Degree of anisotropy}\,(\%) = \frac{E'_{\theta=0} - E'_{\theta=90}}{E'_{\theta=90}} \times 100; \quad (3)$$

The calculated degree of anisotropy (Table 1) shows that the composites with CNW concentration equal to or below 4% had large degree of anisotropy. At 5% concentration, the composites were largely isotropic. Higher CNW concentrations caused more pronounced fiber–fiber and fiber–polymer interactions. These

**Table 1**
Effect of CNW concentration on the degree of anisotropy at 60 °C.

| CNW (wt%) | Degree of anisotropy (%) |
|---|---|
| 1.5 | 76.2 |
| 2 | 39.2 |
| 3 | 38.5 |
| 4 | 23.7 |
| 5 | 2.03 |

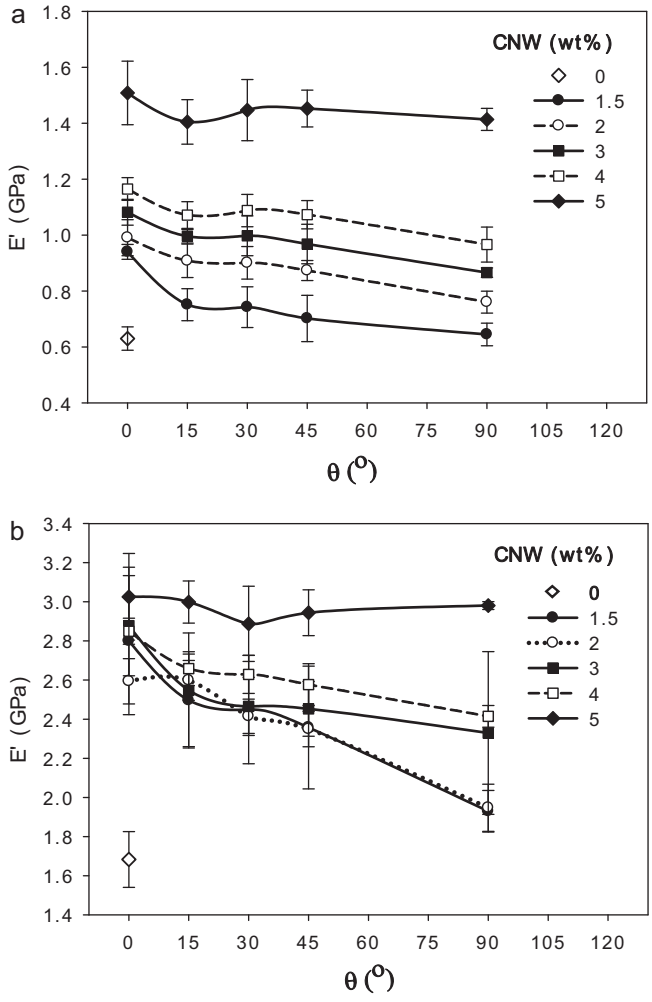


**Fig. 10.** Effects of the CNW orientation and concentration on the storage moduli $E'$ at (a) 60 °C and (b) −10 °C. Error bars represent 1 standard deviation.

interactions in one hand restrained polymer chain mobility which increased the complex viscosity of the composites. On the other hand, the mobility of the fibers was also restricted due to these interactions, especially if a percolated network structure was formed. Therefore the electric field was less effective in orienting the fibers.

Storage moduli ($E'$) of the aligned composites were also compared to their randomly oriented counterparts to further assess the reinforcing effects of the aligned CNWs in different directions. Fig. 11 shows the comparison for the composites containing 1.5% and 2% CNWs. The moduli of the randomly oriented (RO) composites measured at different angles were similar to each other and only the data measured at 0° were plotted in the figure. The moduli of the RO samples fell between the moduli of the 0° and 90° composites and were similar to that of the 45° composite. $E'$ was the lowest at 90° for the aligned composites because the fibers had the weakest reinforcing effect in the transverse direction. The low value of $E'$ at 90° was also partially attributed to the low probability of fiber contacts (forming a fiber network) in the transverse direction as predicted by the excluded volume theory (Balberg, Anderson, Alexander, & Wagner, 1984; Balberg & Binenbaum, 1983; Balberg, Binenbaum, & Bozowski, 1983; Balberg & Bozowski, 1982; Stauffer & Aharony, 1992).

In general, $E'$ of the aligned samples decreased when $\theta$ increased from 0° to 90° due to the fiber orientation. This trend is evident in Figs. 10 and 11. However, Fig. 10 also shows that at high CNW

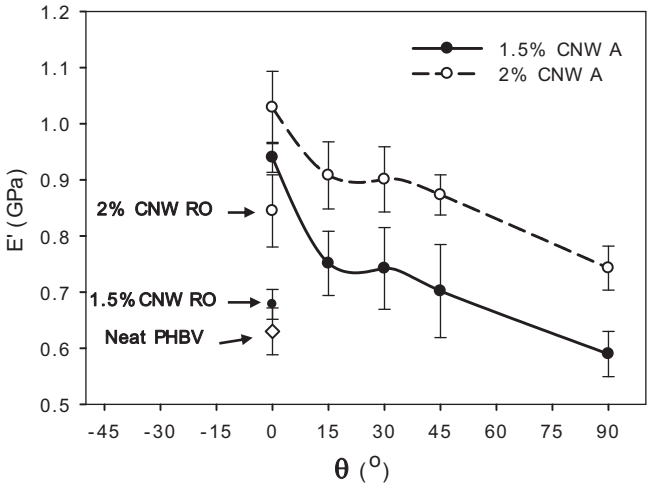


**Fig. 11.** Comparison of $E'$ between the aligned (A) and randomly oriented (RO) PHBV/CNW composites (1.5% and 2% CNWs). Temperature = 60 °C.

concentration (i.e. 5%) $E'$ is relatively constant regardless of the variation of $\theta$. In Fig. 12 $E'$ of the aligned and randomly oriented samples comprising 3%, 4%, and 5% CNWs are compared and the difference in the trend of $E'$ can be clearly seen. The nearly constant $E'$ of the 5% aligned sample indicates that fiber orientation in this sample was negligible. Moreover, at 5% CNW concentration, $E'$ of the randomly oriented sample was 35% lower than that of the corresponding "aligned" sample. Since both samples comprised the same concentration of CNWs and both were virtually isotropic, they should have exhibited similar $E'$. The reason for the abnormally high $E'$ of the "aligned" sample was presumably attributed to the reduced agglomeration of CNWs under the influences of the electric field. The electric field could interfere with the interactions (i.e. hydrogen bonding) between CNWs and therefore hindered their agglomeration (Astrakas, Gousias, & Tzaphlidou, 2011). The improved CNW dispersion in the "aligned" samples could reduce the number of sample defects and increase the interfacial area between the PHBV matrix and CNWs, which contributed to the increase in the moduli of the "aligned" samples.

The improved dispersion of CNWs in the "aligned" PHBV/5 CNW sample was verified with TEM micrographs (Fig. 13). CNW agglomerates were evident for the randomly oriented sample (Fig. 13a)

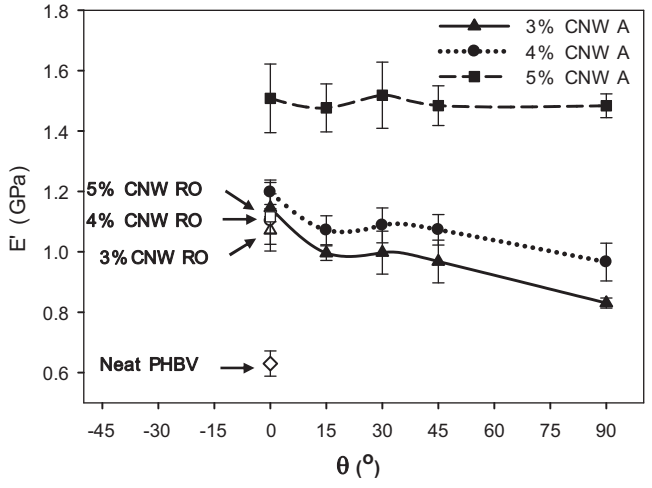


**Fig. 12.** Effect of $\theta$ on $E'$ of the aligned (A) composites. Randomly oriented (RO) samples were shown for comparison. $E'$ was determined at 60 °C.

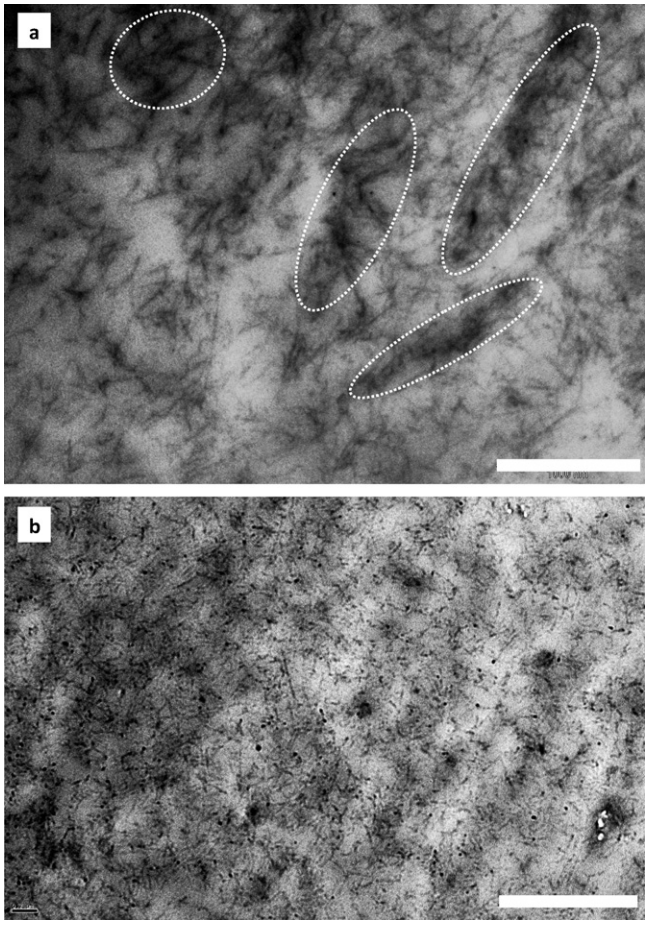


**Fig. 13.** TEM images of (a) randomly oriented and (b) "aligned" PHBV/5 CNW samples. Scale bar is 1 μm. Circled areas indicate CNW agglomerates.

whereas CNW dispersion was largely homogeneous in the "aligned" sample (Fig. 13b).

## 4. Conclusion

This study has demonstrated the successful orientation CNWs in the PHBV matrix using electric field. CNWs were aligned in the direction of the applied electric field. TEM and DMA results showed that CNW concentration strongly influenced the degree of CNW alignment under the electric field. High CNW concentration (>4 wt%) led to high viscosity of the suspension and high restraint on CNW mobility. This caused the electric field to become ineffective in aligning the fibers. The aligned PHBV/CNWs composites showed substantial mechanical anisotropy. The method developed in this paper can be used to prepare CNW nanocomposites with desired directional reinforcement.

## References


Astrakas, L., Gousias, C., & Tzaphlidou, M. (2011). Electric field effects on chignolin conformation. *Journal of Applied Physics*, *109*, 094702–94705.

Azizi Samir, M. A. S., Alloin, F., Sanchez, J.-Y., Kissi, N. El., & Dufresne, A. (2004). Preparation of cellulose whiskers reinforced nanocomposites from an organic medium suspension. *Macromolecules*, *37*, 1386–1393.

Balberg, I., Anderson, C. H., Alexander, S., & Wagner, N. (1984). Excluded volume and its relation to the onset of percolation. *Physical Review B*, *30*, 3933–3942.

Balberg, I., Binenbaum, N., & Bozowski, S. (1983). Anisotropic percolation in carbon-black-polyvinylchloride composites. *Solid State Communications*, *47*(12), 989–992.

Balberg, I., & Binenbaum, N. A. (1983). Computer study of the percolation threshold in a two-dimensional anisotropic system of conducting sticks. *Physical Review B*, *28*(7), 3799–3812.

Balberg, I., & Bozowski, S. (1982). Percolation in a composite of random stick-like conducting particles. *Solid State Communications*, *44*(4), 551–554.

Ballard, D., Holmes, P., & Senior, P. (1987). *NATO ASI Series, Series C: Math. Phys. Sci.* , pp. 293–314.

Bondeson, D., Mathew, A., & Oksman, K. (2006). Optimization of the isolation of nanocrystals from microcrystalline cellulose by acid hydrolysis. *Cellulose*, *13*, 171–180.

Bordel, D., Putaux, J.-L., & Heux, L. (2006). Orientation of native cellulose in an electric field. *Langmuir*, *22*, 4899–4901.

Cranston, E. D., & Gray, D. G. (2003). Birefringence in spin-coated films containing cellulose nanocrystals. *Colloids and Surfaces A: Physicochemical and Engineering Aspects*, *325*, 44–51.

Cranston, E. D., & Gray, D. G. (2006). Formation of cellulose-based electrostatic layer-by-layer films in a magnetic field. *Science and Technology of Advanced Materials*, *7*, 319–321.

Dubief, D., Samain, E., & Dufresne, A. (1999). Polysaccharide microcrystals reinforced amorphous poly(β-hydroxyoctanoate) nanocomposite materials. *Macromolecules*, *32*, 5571–5765.

Ebeling, T., Paillet, M., Borsali, R., Diat, O., Dufresne, A., Cavaillé, J.-Y., et al. (1999). Shear-induced orientation phenomena in suspensions of cellulose microcrystals, revealed by small angle X-ray scattering. *Langmuir*, *15*(19), 6123–6126.

Edgar, C. D., & Gray, D. G. (2003). Smooth model cellulose I surfaces from nanocrystal suspensions. *Cellulose*, *10*, 299–306.

Habibi, Y., & Dufresne, A. (2008). Highly filled bionanocomposites from functionalized polysaccharide nanocrystals. *Biomacromolecules*, *9*, 1974–1980.

Habibi, Y., Heim, T., & Douillard, R. (2008). AC electric field-assisted assembly and alignment of cellulose nanocrystals. *Journal of Polymer Science Part B: Polymer Physics*, *46*(14), 1430–1436.

Jiang, L., Morelius, E., Zhang, J., Wolcott, M. P., & Holbery, J. (2008). Study of the poly(3-hydroxybutyrate-co-3-hydroxyvalerate)/cellulose nanowhisker composites prepared by solution casting and melt processing. *Journal of Composite Materials*, *42*, 2629–2645.

Kimura, F., Kimura, T., Tamura, M., Hirai, A., Ikuno, M., & Horii, F. (2005). Magnetic alignment of the chiral nematic phase of a cellulose microfibril suspension. *Langmuir*, *21*, 2034–2037.

Kvien, I., & Oksman, K. (2007). Orientation of cellulose nanowhiskers in polyvinyl alcohol. *Applied Physics A*, *87*, 641–643.

Li, D., Liu, Z., Al-Haik, M., Tehrani, M., Murray, F., Tannenbaum, R., et al. (2010). Magnetic alignment of cellulose nanowhiskers in an all-cellulose composite. *Polymer Bulletin*, *65*, 635–642.

Mabrouk, A. B., Magnin, A., Belgacem, M. N., & Boufi, S. (2011). Melt rheology of nanocomposites based on acrylic copolymer and cellulose whiskers. *Composites Science and Technology*, *71*, 818–827.

Marcovich, N. E., Auad, M. L., Bellesi, N. E., Nutt, S. R., & Aranguren, M. I. (2006). Cellulose micro/nanocrystals reinforced polyurethane. *Journal of Materials Research*, *21*, 870–881.

Matsuo, M., Sawatari, C., Iwai, Y., & Ozaki, F. (1990). Effect of orientation distribution and crystallinity on the measurement by X-ray diffraction of the crystal lattice moduli of cellulose I and II. *Macromolecules*, *23*(13), 3266–3275.

Nishiyama, Y., Kuga, S., Wada, M., & Okano, T. (1997). Cellulose microcrystal film of high uniaxial orientation. *Macromolecules*, *30*, 6395–6397.

Pirrotta, K. (1993). MS. Thesis. Princeton University.

Rosin, P., & Rammler, E. (1933). The laws governing the fineness of powdered coal. *Journal of the Institute of Fuel*, *7*, 29–36.

Rusli, R., & Eichhorn, S. J. (2008). Determination of the stiffness of cellulose nanowhiskers and the fibre–matrix interface in a nanocomposite using Raman spectroscopy. *Applied Physics Letters*, *93*, 033111.

Sakurada, I., Nukushina, Y., & Ito, T. (1962). Experimental determination of the elastic modulus of crystalline regions in oriented polymers. *Journal of Polymer Science*, *57*, 651–660.

Stauffer, D., & Aharony, A. (1992). *Introduction to percolation theory*. London: Taylor & Francis.

Stucova, A., Davies, G., & Eichhorn, S. J. (2005). The elastic modulus and stress-transfer properties of tunicate cellulose whiskers. *Biomacromolecules*, *6*, 1055–1061.

Sugiyama, J., Chanzy, H., & Maretg, G. (1992). Orientation of cellulose microcrystals by strong magnetic fields. *Macromolecules*, *25*, 4232–4234.

Ten, E., Turtle, J., Bahr, D., Jiang, L., & Wolcott, M. (2010). Thermal and mechanical properties of poly(3-hydroxybutyrate-co-3-hydroxyvalerate)/cellulose nanowhiskers composites. *Polymer*, *51*, 2652–2660.

Ten, E., Jiang, L., Bahr, D. F., Li, B., & Wolcott, M. P. (2012). Effect of cellulose nanowhiskers on mechanical, dielectric and rheological properties of poly(3-hydroxybutyrate-co-3-hydroxyvalerate) (PHBV)/cellulose nanowhiskers (CNW) composites. *Industrial and Engineering Chemistry Research*, *51*, 2941–2951.

Ten, E., Jiang, L., & Wolcott, M. P. (2012). Crystallization kinetics of poly(3-hydroxybutyrate-co-3-hydroxyvalerate)/cellulose nanowhiskers composites. *Carbohydrate Polymers*, http://dx.doi.org/10.1016/j.carbpol.2012.05.076